DOI: 10.1002/cmdc.200600124

Mapping the Fluorophilicity of a Hydrophobic Pocket: Synthesis and Biological Evaluation of Tricyclic Thrombin Inhibitors Directing Fluorinated Alkyl Groups into the P Pocket

Anja Hoffmann-Röder,[b] Eliane Schweizer,[a] Jonas Egger,[a] Paul Seiler,[a] Ulrike Obst-Sander,[c] Björn Wagner,[c] Manfred Kansy,[c] David W. Banner,[c] and François Diederich*[a]

In the completion of our fluorine scan of tricyclic inhibitors to map the fluorophilicity/fluorophobicity of the thrombin active site, a series of 11 new ligands featuring alkyl, alkenyl, and fluoroalkyl groups was prepared to explore fluorine effects on binding into the hydrophobic proximal (P) pocket, lined by Tyr 60A and Trp 60D, His 57, and Leu 99. The synthesis of the tricyclic scaffolds was based on the 1,3-dipolar cycloaddition of azomethine ylides, derived from L-proline and 4-bromobenzaldehyde, with N-(4-fluorobenzyl)maleimide. Introduction of alkyl, alkenyl, and partially fluorinated alkyl residues was achieved upon substitution of a sulfonyl group by mixed Mg/Zn organometallics followed by oxidation/deoxyfluorination, as well as oxidation/reduction/deoxyfluorination sequences. In contrast, the incorporation of perfluoroalkyl groups required a stereoselective nucleophilic addition reaction at the "upper" carbonyl group of the tricycles, thereby yielding scaffolds with an additional OH, F, or OMe group, respectively. All newly prepared inhibitors showed potent biological activity, with inhibitory constants (K_i values) in the range of 0.008–0.163 μM. The X-ray crystal structure of a protein–ligand complex revealed the exact positioning of a difluoromethyl substituent in the tight P pocket. Fluorophilic characteristics are attributed to this hydrophobic pocket, although the potency of the inhibitors was found to be modulated by steric rather than electronic factors.

Introduction

The interest in fluoroorganic molecules is continuously increasing, as many of these compounds are characterized by a unique set of physical and chemical properties that enable their utilization for a variety of different applications ranging from pharmaceutical chemistry to material science.[1] The often intriguing characteristics of fluoroorganic compounds are mainly governed by the combination of the high electronegativity with the small size and low polarizability of fluorine.[2] As a result, the carbon–fluorine bond is highly polar, which in the case of partially fluorinated compounds, leads to strong electrostatic interactions. The latter, together with the similarity in size between H and F often plays a decisive role in the (enhanced) binding of fluorinated, biologically active molecules to their receptors.[3] The most prominent characteristic of fluoroorganic compounds, however, is the very high stability of the C–F bond. This stability, in combination with the modified electronic and chemical properties, has led to a plethora of examples in which favorable modulation of the physicochemical profiles of potential drug candidates has been achieved upon introduction of single F atoms and (per-)fluorinated groups.[1b,4]

To effectively exploit the impact of F on the overall reactivity and stability of biologically active substances, a proper understanding of the molecular recognition features of fluorinated ligands with regard to their receptors is desirable. Therefore, a few years ago we started a program to elucidate the intrinsic properties of fluorophilic or fluorophobic (micro-)environments within an enzyme active site, by systematically exchanging H for F substituents on tricyclic thrombin inhibitors ("F scan").[5] Thrombin was chosen for this investigation because of its rigid and structurally well-defined active site. As a prerequisite for meaningful structure–activity relationships, several X-ray crystal structures have confirmed nearly identical binding geometries for different inhibitors featuring a rigid, tricyclic core.[5a,6] Thus, systematic fluorination of the benzyl ring reaching into the distal (D) pocket (Figure 1) led to the discovery of attractive, orthogonal multipolar C–F···C=O interactions.[5a,b] Further studies, together with database mining,[7] revealed that similar in-

[a] Dr. E. Schweizer, J. Egger, P. Seiler, Prof. Dr. F. Diederich
Laboratorium für Organische Chemie, ETH Zürich
Hönggerberg, HCI, 8093 Zürich (Switzerland)
Fax: (+41) 44-632-1109
E-mail: diederich@org.chem.ethz.ch

[b] Dr. A. Hoffmann-Röder
Institut für Organische Chemie, Johannes Gutenberg-Universität
Duesbergweg 10–14, 55128 Mainz (Germany)

[c] Dr. U. Obst-Sander, Dr. B. Wagner, Dr. M. Kansy, Dr. D. W. Banner
Pharma Research Basel, Discovery Chemistry
F. Hoffmann-La Roche Ltd, 4070 Basel (Switzerland)

Supporting information for this article is available on the WWW under http://www.chemmedchem.org or from the author.

 © 2006 Wiley-VCH Verlag GmbH & Co. KGaA, Weinheim WILEY InterScience DISCOVER SOMETHING GREAT

teractions can also occur with other polar groups, although in the case of thrombin only fluorine substitution resulted in a dramatic increase in the inhibitory potency.[8] We showed that F introduction modulates the lipophilicity of the ligands and decreases the pK_a values of both the tertiary amine center in the tricyclic core and the phenylamidine residue pointing into the selectivity (S1) pocket.[5c,8,9] On the other hand, linear free-energy relationships revealed that decreasing the pK_a value of the phenylamidinium substituent led to significantly weaker binding to thrombin than to the related serine protease trypsin, resulting in an undesirable and unexpected loss in selectivity.[10]

Occupation of the proximal (P) pocket at the thrombin active site by suitably sized alkyl substituents (*i*Pr, *c*Pr, Et) was shown in all investigations to strongly increase both binding affinity and selectivity of the tricyclic lactam-based inhibitors (Figure 1).[5,6,8] This narrow hydrophobic pocket, lined by Tyr60A, Trp60D, His57, and Leu99 (Figure 2) is absent in trypsin. Therefore, at the conclusion of our F-scan, we became interested in exploring the sensitivity of this pocket with respect to steric and electronic modulation of the filling entities, in particular upon introduction of F atoms.

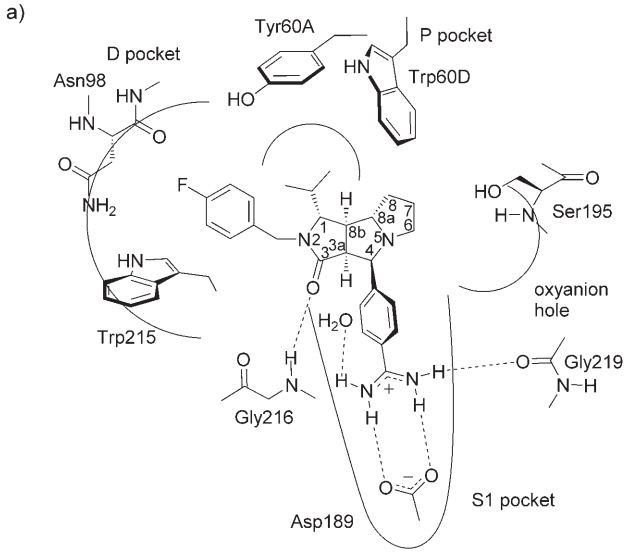

	R^1	R^2
(±)-**1**	H	$CH(CH_3)_2$
(±)-**2**	H	CH_2CH_3
(±)-**3**	H	$CH=CH_2$
(±)-**4**	H	$(CH_2)_2CH_3$
(±)-**5**	H	$CH_2CH=CH_2$
(±)-**6**	H	CH_2F
(±)-**7**	H	CHF_2
(±)-**8**	H	CH_2CH_2F
(±)-**9**	H	CH_2CHF_2
(±)-**10**	OH	CF_3
(±)-**11**	OMe	CF_3
(±)-**12**	CF_3	OMe

Figure 1. a) Representation of the binding mode of tricyclic inhibitor (±)-**1** in the active site of thrombin. b) Inhibitors (±)-**1**–(±)-**12** prepared to investigate the fluorophilicity/fluorophobicity of the tight P pocket. Only the (3a*S*,4*R*,8a*S*,8b*R*)-configured enantiomers display high potency.[5,6]

We describe herein the synthesis of the tricyclic lactam-based inhibitors (±)-**1**–(±)-**12** featuring different alkyl, alkenyl, and fluoroalkyl groups directed towards the P pocket. Their biological activity and physicochemical properties (pK_a and log *D*) are compared, not only to gain a deeper insight into the "actual size" of the narrow P pocket and its (fluorinated) filling entities, but also to elucidate polar interactions between alkenyl and fluoroalkyl groups of the ligands and the hydrophobic amino acids lining the pocket.

Results and Discussion

Synthesis of the Inhibitors

The racemic thrombin inhibitors (±)-**1**–(±)-**12** (Figure 1) were obtained following previously reported protocols.[5,6] The synthesis of the difluoromethylated derivative (±)-**7** is shown in Scheme 1, whereas the preparation of the other partially fluorinated ligands, and the alkylated reference compounds, is reported in the Supporting Information (SI). The syntheses of the perfluoroalkylated inhibitors (±)-**10**–(±)-**12** are illustrated in Scheme 2. The tricyclic inhibitor scaffold was assembled in a 1,3-dipolar cycloaddition reaction starting from readily available *N*-(4-fluorobenzyl)maleimide (**13**), commercial 4-bromobenzaldehyde (**14**), and L-proline (**15**).[5,6] The resulting diastereomeric pairs of enantiomers, *endo*,*trans*-configured tricycle (±)-**16** and the *exo*,*trans*-configured cycloadduct (±)-**17**, were readily separated by column chromatography on silica gel. Compound (±)-**16** was transformed into hydroxylactam (±)-**18** by regio- and stereoselective reduction and converted into sulfone (±)-**19**, thereafter.[5b] Its sulfonyl group was then replaced stereoselectively by an ethyl ((±)-**20**), vinyl ((±)-**21**), propyl ((±)-**22**), or allyl ((±)-**23**) group using the corresponding Grignard reagent in the presence of $ZnCl_2$. Subsequent Br/CN exchange, followed by a Pinner reaction,[11] led to the four reference inhibitors (±)-**2**–(±)-**5**, directing alkenyl and alkyl groups towards the P pocket (SI). Ozonolysis of olefin (±)-**21** and reductive workup with Me_2S gave aldehyde (±)-**24**, which was directly subjected to deoxyfluorination with diethylaminosulfur trifluoride[12] (DAST), furnishing the difluoromethylated intermediate (±)-**25** (Scheme 1). The conversion of (±)-**25** into inhibitor (±)-**7** was accomplished by Br/CN exchange to (±)-**26** and Pinner reaction (Scheme 1). Analogously, target compound (±)-**9** was prepared starting from the allyl derivative (±)-**23**, whereby the monofluorinated adducts were obtained from (±)-**21** and (±)-**23**, respectively, through reduction of the corresponding aldehydes and deoxyfluorination with DAST. The last steps towards the phenylamidinium salts (±)-**6** and (±)-**8** again followed the synthetic route described above (SI).

While the introduction of the alkyl and alkenyl substituents using the corresponding Mg/Zn organometallics proceeded smoothly, only few comparable substitution reactions using perfluoroalkylated nucleophiles have been reported to date.[13] However, our attempts to accomplish such reactions on the tricyclic inhibitor scaffold failed. Instead, incorporation of a CF_3 group, such as in (±)-**27**, required the stereoselective nucleophilic addition of CF_3SiMe_3[14] to the "upper" carbonyl group of

 © 2006 Wiley-VCH Verlag GmbH & Co. KGaA, Weinheim

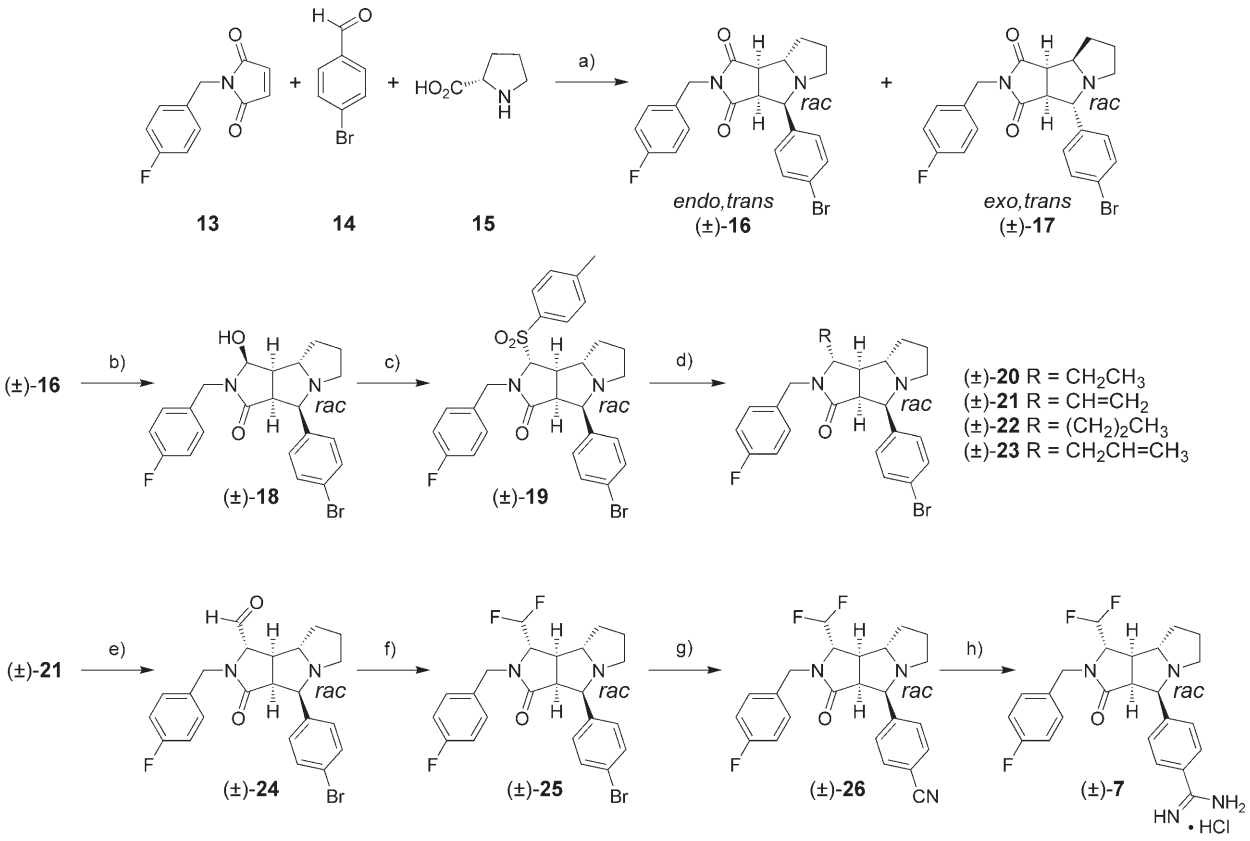

Scheme 1. Synthesis of the partially fluorinated inhibitor (±)-**7**: a) CH_3CN, 80 °C, 16 h, (±)-**16** (44%), (±)-**17** (42%); b) $Li[Et_3BH]$, CH_2Cl_2, −78 °C, 2 h; c) 4-toluenesulfinic acid, $CaCl_2$, CH_2Cl_2, 25 °C, 6 d, 64% (from (±)-**16**); d) $ZnCl_2$, RMgX, CH_2Cl_2, 0 °C→25 °C, 16 h, (±)-**20** (44%), (±)-**21** (98%), (±)-**22** (53%), (±)-**23** (61%); e) 1. O_3, TFA, CH_2Cl_2, −78 °C, 20 min; 2. Me_2S, CH_2Cl_2, 25 °C, 16 h; f) DAST, CH_2Cl_2, −78 °C→25 °C, 2 h, (16%), (from (±)-**21**); g) CuCN, DMF, 180 °C, 22 h, 42%; h) 1. MeOH, HCl(g), CH_2Cl_2, 4 °C, 29 h; 2. NH_3, MeOH, 65 °C, 3 h, (68%). DAST = diethylaminosulfur trifluoride, DMF = *N*,*N*-dimethylformamide, TFA = trifluoroacetic acid. Only *endo*,*trans*-configured adducts led to active inhibitors.[5a,6] *Exo* and *endo* refer to the orientation of the 4-bromophenyl substituent at C(4) with respect to the bicyclic perhydropyrrolo[3,4-c]pyrrole scaffold, and *cis* and *trans* to the position of this 4-bromophenyl ring with respect to the configuration of C(8a) at the fusion of the two pentagons in the perhydropyrrolizidine bicycle (for atom numbering, see Figure 1).

the tricyclic imide (±)-**16** (Scheme 2). As expected,[15] attack of the CF_3 nucleophile occurred diastereoselectively from the less shielded *exo* side of the tricycle.[16] Likewise, nucleophilic addition of $C_2F_5SiMe_3$[14b,17] and C_3F_7MgBr,[18] prepared in situ from C_3F_7I and EtMgBr, exclusively furnished the corresponding lactams as *exo* diastereomers (SI).

Conversion of adduct (±)-**27** into inhibitor (±)-**10** by Br/CN exchange ((±)-**28**) and Pinner reaction proceeded smoothly. In contrast, Br/CN exchange of the C_2F_5 and C_3F_7 substituted bromides only resulted in excision of the perfluoroalkyl residues under formation of imide (±)-**16**. In these cases, the enhanced acidity of the HO group presumably favors deprotonation over nitrile formation,[19] leading to fragmentation under regeneration of the carbonyl group by loss of HF and $F_2C{=}CF_2$ or $F_3CFC{=}CF_2$, respectively.

Moreover in accordance to literature precedence,[20] the CF_3 group strongly stabilizes the adjacent tertiary alcohol which, in our case, resisted most deoxygenation procedures, except for deoxyfluorination. Thus, treatment of nitrile (±)-**28** with DAST furnished a mixture of two diastereomeric fluorolactams (±)-**29** and (±)-**30**, which were separated by column chromatography on silica gel. Configurational assignment of the two CF_3 substituted fluorolactams was possible by solving the X-ray crystal structure of (±)-**30** (SI). Interestingly, after Pinner reaction of compound (±)-**29**, only the MeO substituted inhibitor (±)-**12** was obtained instead of the expected fluoro derivative. Its stereoselective formation can be explained by loss of F- and subsequent attack of the resulting *N*-acyliminium ion by MeOH from the less hindered *exo* side of the tricycle. ^1H and ^{13}C NMR spectroscopic analysis of diastereomer (±)-**11**, accessible from hydroxylactam (±)-**28** upon methylation (→ (±)-**31**) and Pinner reaction, and comparison to the data obtained for (±)-**12** confirmed the configurational assignment.

X-ray Crystallography

Various small-molecule crystallographic analyses are described in the SI. They support the configurational assignments made for the tricyclic inhibitors and feature a series of surprisingly short F···F, F···O(ether), and F···N(nitrile) contacts with interatomic distances between 2.94 and 3.15 Å. In addition, a co-crystal structure of the productive, (3a*S*,4*R*,8a*S*,8b*R*)-configured enantiomer of inhibitor (±)-**7** in complex with thrombin (inhibition constant $K_i = 22$ nM, Table 1) was obtained at 1.31 Å resolution (PDB-code: 2CN0, Figure 2a).

 © 2006 Wiley-VCH Verlag GmbH & Co. KGaA, Weinheim

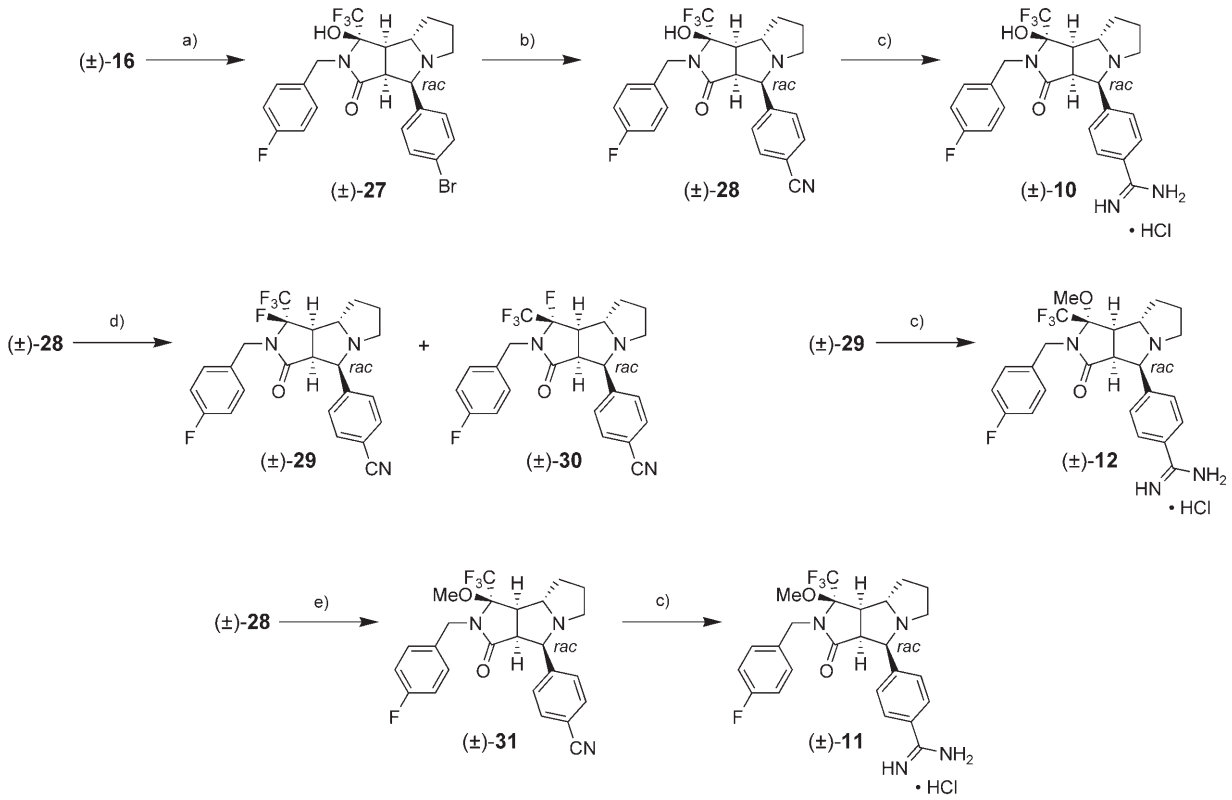

Scheme 2. Synthesis of the trifluoromethylated inhibitors (±)-**10**–(±)-**12**: a) CsF, CF_3SiMe_3, THF, 0 °C→10 °C, 6 h, (64%); b) CuCN, DMF, 180 °C, 16 h, (73%); c) 1. MeOH, HCl(g), CH_2Cl_2, 4 °C, 29–36 h; 2. NH_3, MeOH, 65 °C, 3 h, (±)-**10** (53%), (±)-**11** (51%), (±)-**12** (41%); d) DAST, CH_2Cl_2, −78 °C→25 °C, 2 h, (±)-**29** (43%), (±)-**30** (40%); e) 18-Crown-6, MeI, NaH, THF, 1 h, 25 °C, quant.

Table 1. Biological activities and physicochemical properties of thrombin inhibitors.

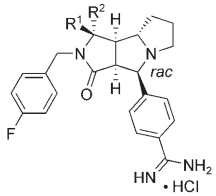

	R^1	R^2	K_i [μM][a]	Sel.[b]	p$K_{a1\ exp}$[c]	p$K_{a1\ calc}$[d]	pK_{a2}[c]	log D[e]
(±)-**1**[f,g]	H	$CH(CH_3)_2$	0.005	413	6.52	–	n.d.[h]	−1.08
(±)-**2**[f]	H	CH_2CH_3	0.014	501	6.27	–	11.15	−0.79
(±)-**3**[f]	H	$CH{=}CH_2$	0.008	835	6.02	–	11.15	−0.90
(±)-**4**[f]	H	$(CH_2)_2CH_3$	0.078	70	6.16	–	n.d.	−0.59
(±)-**5**[f]	H	$CH_2CH{=}CH_2$	0.036	156	6.19	–	n.d.	−0.91
(±)-**6**[f]	H	CH_2F	0.028	407	5.95	7.27	10.98	−1.09
(±)-**7**[f]	H	CHF_2	0.022	297	5.61	6.93	11.07	−1.16
(±)-**8**[f]	H	CH_2CH_2F	0.012	395	6.08	7.56	10.96	−1.24
(±)-**9**[f]	H	CH_2CHF_2	0.038	104	6.00	7.42	11.32	−1.01
(±)-**10**[f]	OH	CF_3	0.163	30	5.52	6.13	10.96	−0.55
(±)-**11**[f]	OMe	CF_3	0.018	160	5.16	5.98	11.19	−0.05
(±)-**12**[f]	CF_3	OMe	0.022	297	4.88	5.98	n.d.	−0.28

[a] The uncertainty of the measured K_i values is ±20%. [b] Selectivity (Sel.) = K_i(trypsin)/K_i(thrombin). [c] p$K_{a1\ exp}$: tertiary amine in the tricyclic core; pK_{a2}: phenylamidinium. Accuracy of the pK_a measurements: ±0.1 pK_a units. [d] p$K_{a1\ calc}$: calculated with ACD/pK_a version 8.19.[25] [e] Accuracy of the log D measurements: ±0.1 log D units. [f] Only the (3a*S*,4*R*,8a*S*,8b*R*)-configured enantiomer is bound, as determined from crystal structure analyses.[5a,6,8] [g] From [5a]. [h] n.d. = Not detectable due to poor UV absorption.

The occupancy of the various subpockets is as expected, with the phenylamidinium residue filling the S1 pocket, the 4-fluorobenzyl moiety the D pocket, and the difluoromethyl group the narrow P pocket. In agreement with previous X-ray data on co-crystals,[8] filling the P pocket shifts the loop including Leu 99 and Asn 98 away from the bound ligand. As a result,

 © 2006 Wiley-VCH Verlag GmbH & Co. KGaA, Weinheim

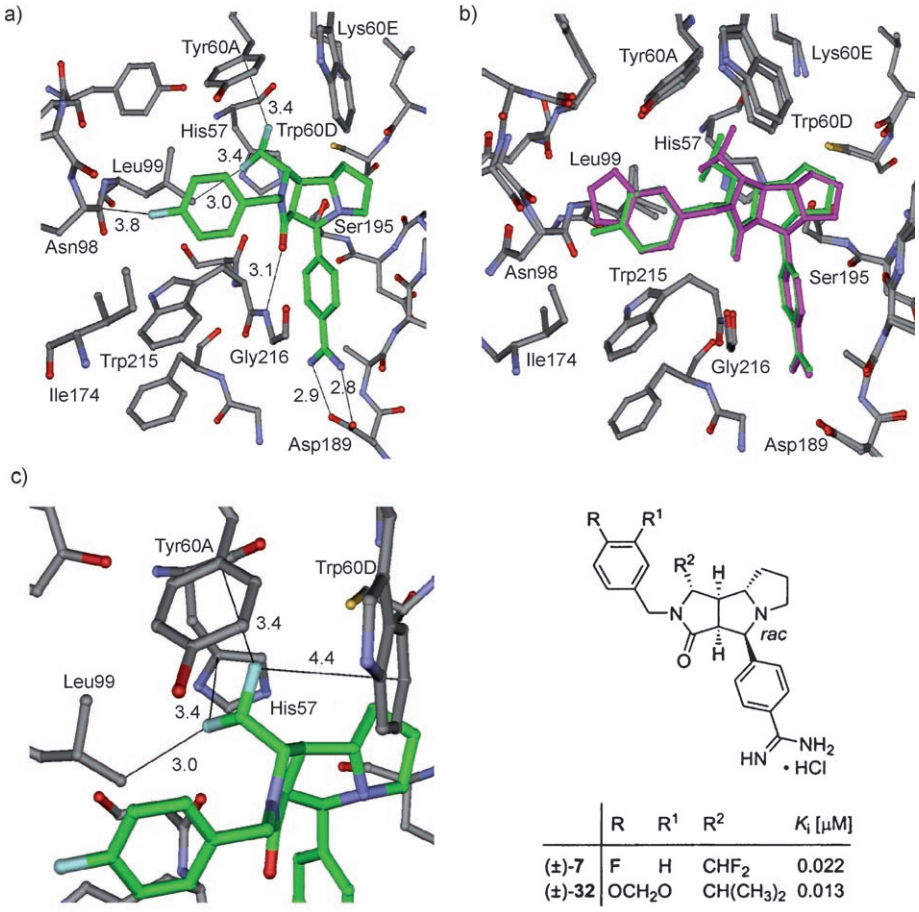

Figure 2. a) Inhibitor (±)-**7** in the active site of thrombin as determined by X-ray crystallographic analysis. Only the (3a*S*,4*R*,8a*S*,8b*R*)-configured enantiomer is bound. b) Superimposition of the co-crystal structures of (±)-**7** and (±)-**32**, showing the slight displacement of the residues directed into the P pocket. c) Binding mode of the difluoromethyl moiety of (±)-**7** in the P pocket of thrombin. Distances shown are in Å. Color code: C-skeleton of inhibitor (±)-**7**: green, C-skeleton of inhibitor (±)-**32**: pink, C-skeleton of the proteins: grey, O-atoms: red, N-atoms: blue, F-atoms: light green, S-atoms: yellow.

the fluorine on the benzyl ring in the D pocket is positioned 3.8 Å away from the C atom of the backbone C=O of Asn98. This distance is too large for efficient orthogonal dipolar C–F···C=O interactions.[5a,7] An overlay of this co-crystal structure and the one in complex with (±)-**32**[6b] shows a nearly constant overall binding geometry (Figure 2b). Yet, a slight displacement of the substituent pointing into the P pocket can be observed. This causes the difluoromethyl residue of (±)-**7** to be oriented more towards the side chain of Leu99, and thus further away from the electron cloud of the indole ring of Trp60D, as was the case for the isopropyl group of (±)-**32** (for distances see Figure 2c). The F atoms of the CHF_2 residue in (±)-**7** now appear closer to the aromatic rings of His57 and Tyr60A than the corresponding C atoms of (±)-**32** because of this shift (SI). We would like to emphasize at this point that the observed shifts can be taken into account to explain the different binding affinities obtained for the various inhibitors. However, these displacements are very slight and therefore it can be stated in general, as in previous work,[5,8] that the overall geometry of the active site and especially of the residues of the P pocket (Tyr60A, Trp60D, His57, and Leu99) does not change upon variation of the substituents of the ligand that fill the four binding pockets. A Newman projection of inhibitor (±)-**7**, as determined from the co-crystal structure, reveals one perfectly staggered conformation of the F atoms with respect to N(2) and C(8b) of the tricyclic core (SI). The two alternative staggered conformations are not observed. According to computer modeling using MOLOC,[21] they would lead to a repulsive contact between an F atom and the 4-fluorobenzyl ring of the inhibitor (with F···C distances of < 2.5 Å).

Biological Results

The inhibition constants K_i for all of the newly synthesized compounds (±)-**2** to (±)-**12** toward thrombin and trypsin were determined in a chromogenic enzymatic assay as previously described.[22] The K_i values of the non-fluorinated ((±)-**2**–(±)-**5**) and partially fluorinated derivatives ((±)-**6**–(±)-**9**) varied between 0.008 and 0.078 μM, indicating the potent biological activity of these compounds (Table 1). This suggests that the lipophilic P pocket represents a suitable environment for partially fluorinated residues, which can be accommodated without a significant loss in binding activity.[23]

However, the observed selectivities (K_i(trypsin)/K_i(thrombin)) for thrombin over trypsin range from excellent values for the ethyl ((±)-**2**: 501) and vinyl ((±)-**3**: 835) substituted derivatives to rather low values for propyl ((±)-**4**: 70), allyl ((±)-**5**: 156), and difluoroethyl ((±)-**9**: 104). Apparently, the accommodation of the larger substituents within the tight P pocket is less optimal, as is also reflected in the slight increase in their inhibition constants ($K_i = 0.078$ μM for (±)-**4**, 0.036 μM for (±)-**5**, and 0.038 μM for (±)-**9**).

A molecular modeling analysis[21] suggests indeed the occurrence of repulsive interactions between the propyl chain of (±)-**4** in its energetically more favorable *anti* conformation and the residues lining the P pocket. Thus, modification (difluoromethyl → *n*-propyl) of the inhibitor in the co-crystal structure (Figure 2) and subsequent energy minimization with the conformation of the protein kept fixed, resulted in a predicted change to the *gauche* conformation for the C(ring)–CH_2–CH_2–

 © 2006 Wiley-VCH Verlag GmbH & Co. KGaA, Weinheim

CH_3 fragment, which could account for the observed increase in the K_i value (SI).

The perfluoroalkylated derivatives also showed potent inhibition of thrombin, with K_i values of 0.163 μM for (±)-**10**, 0.018 μM for (±)-**11**, and 0.022 μM for (±)-**12**, respectively. Molecular modeling analyses (Figure 3) suggest that both the *exo* and the *endo* substituent of the lactam ring penetrate the P pocket. Different size and solvation requirements of the pairs of substituents in the three ligands lead to different binding geometries in the rigid P pocket, affecting also the interactions within the D pocket. The large difference in affinity between alcohol (±)-**10** and methyl ether (±)-**11** reflects the high energetic costs arising from the desolvation of the HO group and the absence of a suitable hydrogen bond acceptor within the P pocket. Moreover, compound (±)-**10** features a very low selectivity for thrombin over trypsin (factor of 30), whereas this ratio was significantly increased for the methyl ethers (±)-**11** and (±)-**12** (160 and 297, respectively).

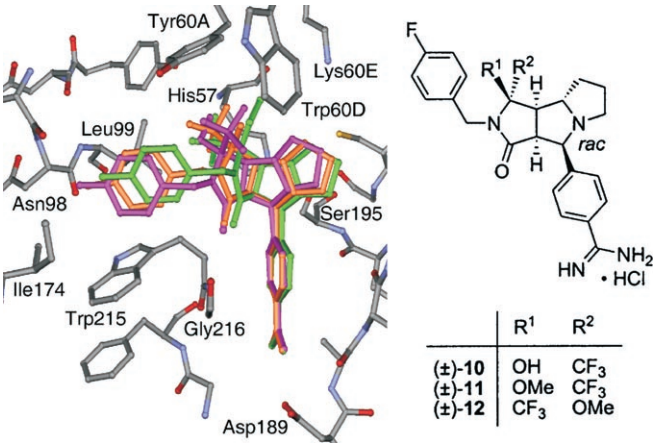

Figure 3. Superimposition of the trifluoromethylated inhibitors (±)-**10** to (±)-**12** showing the differences in binding geometries imposed by the constraints of the rigid, apolar P pocket. Color code: C-skeleton of (±)-**10**: orange, C-skeleton of (±)-**11**: green, C-skeleton of (±)-**12**: pink, C-skeleton of the protein: grey, O-atoms: red, N-atoms: blue, S-atom: yellow.

Interestingly, fluorine atoms in the substituents filling the P pocket still have a remarkable effect on the pK_a values of the tertiary amine center in the tricyclic skeleton, five or more bonds away (Table 1).[5c,8,9] While the pK_a values of the tertiary N center in the alkylated and alkenylated lactams vary between 6.0 and 6.5, introduction of the CHF_2 substituent lowers this value to 5.6 and, in the presence of both MeO and CF_3 substituents, values of 4.9 and 5.2 are measured. These data document once more the substantial σ-withdrawing effects of fluorine atoms even on remote basic/acidic centers.[1c,e,24] Whereas the pK_{a1} values of the fluorinated inhibitors calculated with the ACD software[25] (p$K_{a1\ calc}$, Table 1) are reproducing the general trend of the values obtained experimentally (p$K_{a1\ exp}$), however, they are found approximately 1 to 1.5 pK_a units too high. For the phenylamidine moiety values of about pK_{a2} = 11.6 are predicted for all compounds. Whereas the introduction of CF_3 groups (in (±)-**10**–(±)-**12**) increases the lipophilicity of the ligands, as measured by the logarithmic distribution coefficient log *D*, the introduction of partially fluorinated alkyl residues (in (±)-**6**–(±)-**9**) leads to an "inverse fluorine effect",[8,9] that is, a slight increase in the hydrophilicity (Table 1). The origin of the "inverse fluorine effect" that we also observed in previous studies,[8,9] is currently the subject of a comprehensive investigation.

Conclusions

To investigate the affinity of fluorinated residues for the tight and rigid hydrophobic P pocket of thrombin, we prepared a series of tricyclic inhibitors featuring partially and perfluorinated alkyl groups and compared their binding potency to that of alkyl and alkenyl substituted analogues. Overall, a series of inhibitors with similarly high potency was obtained, with K_i values ranging from 0.08 μM to 0.163 μM, supporting the postulate that the P pocket lined by Tyr 60A, Trp 60D, Leu 99, and His 57 possesses both hydrophobic and fluorophilic characteristics. The requirement for steric fit between the P pocket and the penetrating substituent leads to small adjustments of the overall ligand binding geometry. Thus, the crystal structure of the co-crystal of thrombin and (±)-**7** (K_i = 0.022 μM) shows that the CHF_2 substituent turns away from the π-electron rich indole ring of Trp 60D to prevent electrostatic repulsion. With increasing substituent size, binding affinity weakens. To prevent steric clashes, substituents occupying the P pocket may adopt less favorable conformations as proposed for the *n*-propyl derivative (±)-**4** (K_i = 0.078 μM) based on computer modeling. Binding is further weakened if accompanied by unfavorable desolvation, as shown for alcohol (±)-**10** (K_i = 0.163 μM). This study therefore confirms that the introduction of fluoroalkyl substituents into tight lipophilic pockets lined by electron-rich aromatic rings neither increases nor decreases binding affinity substantially, when compared to similarly sized alkyl and alkenyl residues. However, taking into account the frequently advantageous effects on physicochemical properties, an overall benefit may result in many lead optimization projects from the decoration of ligands with fluoroalkyl residues to occupy apolar aromatic pockets.

With this paper we conclude our fluorine scan of the tricyclic thrombin inhibitors which has helped to identify favorable sites for H/F substitutions, in terms of binding and changes in physicochemical properties.[5,8,9] H/F substitution of the phenylamidinium needle in the S1 pocket reduces binding affinity, as does the introduction of fluorine atoms in highly hydrophilic regions of the active site, such as the oxyanion hole (O). On the other hand, specific fluorine introduction into the benzyl residue occupying the D pocket strengthens binding through multipolar C–F···C=O interactions and the hydrophobic P pocket is also shown in this study to be quite fluorophilic. Based on these conclusions, we suggest systematic fluorine scans of ligands as a promising strategy in lead optimization not only to enhance physicochemical properties but also to strengthen protein–ligand binding interactions.

 © 2006 Wiley-VCH Verlag GmbH & Co. KGaA, Weinheim

Experimental Section

General: Solvents and reagents were reagent-grade, purchased from commercial suppliers, and used without further purification unless otherwise stated. THF was freshly distilled from sodium benzophenone ketyl, CH_2Cl_2 from CaH_2. HCl gas was dried with conc. H_2SO_4. If not mentioned otherwise, all products were dried under high vacuum (10^{-2} Torr) before analytical characterization. Column chromatography (CC): SiO_2-60 (230–400 mesh, 0.040–0.063 mm) from *Fluka*. TLC: SiO_2-60 F_{245} (on glass) *Merck*, visualization by UV light at 245 nm and staining with a solution of $KMnO_4$ (1.5 g), K_2CO_3 (10 g), 5% NaOH (2.5 mL) in H_2O (150 mL); a solution of anisaldehyde (6.8 mL), concentrated H_2SO_4 (9.2 mL), and acetic acid (2.8 mL) in EtOH (250 mL); or a solution of ninhydrin (0.3 g) in butanol (100 mL) and glacial acetic acid (3 mL). mp.: Büchi-510 apparatus; uncorrected. IR Spectra: Perkin–Elmer Spectrum BX FTIR System spectrometer (ATR-unit, Attenuated Total Reflection, Golden Gate). NMR spectra (^1H, ^{13}C, ^{19}F): Varian Gemini-300, and Bruker ARX-300; spectra were recorded at 25 °C with solvent peak or $CFCl_3$ as reference, respectively. In the ^1H and ^{13}C NMR spectra of compounds (±)-**2**, (±)-**3**, (±)-**4**, (±)-**8**, (±)-**9**, (±)-**10**, (±)-**25**, (±)-**26**, (±)-**29**, (±)-**36**, some resonances overlap or are buried under the solvent peak. The exchangeable amidinium protons were not observed in ^1H NMR spectra recorded in CD_3OD. High-resolution MALDI mass spectra (HRMS): IonSpec Ultima, 2,5-dihydroxybenzoic acid (DHB) as matrix; molecular ions (M^+) reported for phenylamidinium salts refer to the corresponding phenylamidine derivatives. The nomenclature was generated with the computer programs AUTONOM (Beilstein) and ACD-Name (ACD/Labs).

Determination of inhibition constants: The affinity of thrombin inhibitors was determined according to previously described procedures (chromogenic substrate S-2238).[22] An exhaustive protocol of the binding assay used in this study is also provided.[22b]

Determination of pK_a values: The determination of pK_a values was performed by potentiometric titration following a protocol previously described.[5c]

Determination of log *D* values: The logarithmic distribution coefficient log *D* was determined by a high-throughput (HT) screening method as previously described.[5c]

General procedure A for the replacement of the sulfonyl group: The corresponding Grignard reagent (1.20 mmol) was added to a solution of $ZnCl_2$ (0.66 mmol; as a 1 M solution in Et_2O) in dry CH_2Cl_2 (6 mL), and the mixture stirred under Ar for 30 min. A solution of sulfone (0.60 mmol) in dry CH_2Cl_2 (6 mL) was slowly added under ice cooling and the mixture stirred for 16 h at 25 °C. After addition of 1 M HCl (10 mL), the mixture was neutralized with saturated aqueous $NaHCO_3$ (10 mL) and extracted with CH_2Cl_2. The organic phases were dried (Na_2SO_4), the solvent evaporated in vacuo, and the residue purified by CC (SiO_2; cyclohexane/AcOEt 1:1, 2:1, or 3:2).

General procedure B for the ozonolysis of an olefin: Ozone was bubbled through a solution of olefin (1.25 mmol) and TFA (1.88 mmol) in CH_2Cl_2 (60 mL), cooled to −78 °C until the solution colored blue (20 min). Oxygen was then bubbled through the solution for 30–45 min, before dimethyl sulfide (5 mL) was added, the mixture warmed to 25 °C, and stirred for 5–16 h. The solvent was evaporated in vacuo, the residue dissolved in CH_2Cl_2 (20 mL), and washed with water. The combined organic phases were dried (Na_2SO_4) and concentrated in vacuo. The residue was used without further purification.

General procedure C for the fluorination with DAST: A solution of alcohol or aldehyde (1.25 mmol) in dry CH_2Cl_2 (5 mL) was cooled under Ar to −78 °C, before DAST (5.00 mmol) was added. After 30 min, the mixture was warmed to 25 °C and stirred for 2–16 h. MeOH (2 mL) was added and the mixture poured into ice-cold, saturated aqueous $NaHCO_3$ solution and stirred for 30 min, then extracted with CH_2Cl_2. The combined organic phases were dried (Na_2SO_4), the solvent evaporated, and the residue purified by CC (SiO_2; cyclohexane/AcOEt 1:1, 2:1 or AcOEt/CH_2Cl_2 2:1).

General procedure D for the reduction of an alcohol with $NaBH_4$: The aldehyde (1.08 mmol) was dissolved in a mixture of EtOH/H_2O (5:1, 36 mL) and cooled to 0 °C. $NaBH_4$ (1.08 mmol) was added, the mixture slowly warmed to 25 °C and stirred for 15–16 h. AcOEt (50 mL) and saturated aqueous NaCl solution (40 mL) were added, and the aqueous phases were extracted with CH_2Cl_2. The combined organic phases were dried (Na_2SO_4) and concentrated in vacuo. The residue was used without further purification.

General procedure E for the conversion of an aryl bromide into an aryl nitrile: A well-degassed suspension of CuCN (1.58 mmol) in dry DMF (7 mL) was heated at reflux under Ar for 30–60 min, before a degassed solution of bromide (0.39 mmol) in dry DMF (3 mL) was added and the mixture stirred for 16–22 h. The solvent was evaporated in vacuo, the residue dissolved in CH_2Cl_2 (10 mL) and concentrated aqueous NH_4OH solution (5 mL) was added. The mixture was stirred at 25 °C for 1 h, the blue aqueous phase removed, the organic phases washed with solutions of concentrated aqueous NH_4OH (10 mL) and saturated aqueous NaCl (10 mL), dried (Na_2SO_4), and the solvent removed in vacuo. The residue was purified by CC (SiO_2; cyclohexane/AcOEt 1:1, 3:2 or CH_2Cl_2/AcOEt 2:1).

General procedure F for the preparation of amidinium salts by the Pinner reaction: Dry HCl gas was bubbled at 0 °C for 10 min into a solution of the nitrile (0.15 mmol) in dry CH_2Cl_2 (0.9 mL) and dry MeOH (1.7 mL). The mixture was stored at 4 °C for 29–36 h, then the solvent was removed in vacuo. The residue was precipitated with Et_2O, filtrated, and dried in high vacuum, then dissolved in NH_3 (2 mL; as a 7 N solution in MeOH) and stirred for 3 h at 65 °C. The solvent was evaporated in vacuo and the residue purified by CC (SiO_2; CH_2Cl_2/MeOH 9:1).

General procedure G for the nucleophilic trifluoromethylation using CF_3SiMe_3: To a mixture of the imide (0.5 mmol) and CsF (20 mol-%) in dry THF (10 mL) under Ar at 0 °C, CF_3SiMe_3 (2 mmol) was slowly added by syringe. The mixture was stirred for 6 h at 0 °C to 10 °C and after complete transformation (TLC), the mixture was hydrolyzed with 1 M HCl (10 mL) at 0 °C and stirred for an additional 30 min. The organic phases were separated and washed with saturated aqueous $NaHCO_3$ solution, the combined aqueous phases were extracted with AcOEt, and the combined organic phases were washed with saturated aqueous NaCl solution and dried ($MgSO_4$). The solvent was evaporated in vacuo and the residue purified by CC (cyclohexane/AcOEt 3:1).

General procedure H for the nucleophilic perfluoroethylation using $C_2F_5SiMe_3$: To a mixture of the imide (0.5 mmol) and CsF (15 mol-%) in dry THF (10 mL) under Ar at 0 °C, $C_2F_5SiMe_3$ (2 mmol) was added rapidly via syringe. After 30 min at 0 °C, an additional amount of CsF (15 mol-%) was added and the mixture was stirred for 6–8 h at 0 °C to 10 °C. After complete transformation (TLC), the reaction mixture was hydrolyzed by addition of 1 M HCl (10 mL) at 0 °C and stirred for an additional 30 min. The organic phase was separated and washed with saturated aqueous $NaHCO_3$ solution, the combined aqueous phases were extracted with AcOEt, and the

 © 2006 Wiley-VCH Verlag GmbH & Co. KGaA, Weinheim

combined organic phases were washed with saturated aqueous NaCl solution and dried ($MgSO_4$). The solvent was evaporated in vacuo and the residue purified by CC (cyclohexane/AcOEt 3:1).

General procedure I for the nucleophilic perfluoropropylation using C_3F_7MgBr: Ethylmagnesium bromide (0.6 mmol; as a 3 M solution in Et_2O) was added dropwise to a solution of C_3F_7I (1 mmol) in dry THF (6 mL) under Ar cooled to −45 °C and protected from light. The mixture was stirred at −45 °C for 30 min, before a solution of the imide (0.25 mmol) in dry THF (4 mL) was added dropwise by syringe. The reaction temperature was left to rise slowly to 10 °C (2–4 h), and the mixture was hydrolyzed with 1 M HCl (10 mL). The organic phase was separated and washed with saturated aqueous $NaHCO_3$ solution, the combined aqueous phases were extracted with AcOEt, and the combined organic phases were washed with saturated aqueous NaCl solution and dried ($MgSO_4$). The solvent was evaporated in vacuo and the residue purified by CC (cyclohexane/AcOEt 3:1).

(1*RS*,3a*SR*,4*RS*,8a*SR*,8 b*RS*)-4-(4-Bromophenyl)-2-(4-fluorobenzyl)-1-vinyloctahydropyrrolo[3,4-*a*]pyrrolizin-3-one ((±)-21): *General procedure A*, starting from $ZnCl_2$ (1.9 mL, 1.9 mmol; as a 1 M solution in Et_2O), vinylmagnesium bromide (3.4 mL, 3.4 mmol; as a 1 M solution in Et_2O), and sulfone (±)-**19** (945 mg, 1.6 mmol) in CH_2Cl_2 (15 mL) gave (±)-**21** (723 mg, 98%) as a yellow oil. ^{1}H NMR (300 MHz, $CDCl_3$): δ = 7.40, 7.24 (AA′BB′, J = 8.6 Hz, 4H), 7.07–7.02 (m, 4H), 5.61 (ddd, J = 17.1, 10.0, 8.7 Hz, 1H), 5.24 (dd, J = 10.0, 1.3 Hz, 1H), 5.18 (dd, J = 17.1, 1.3 Hz, 1H), 4.78, 3.68 (AB, J = 14.5 Hz, 2H), 4.04 (d, J = 8.4 Hz, 1H), 3.72 (dd, J = 8.7, 3.7 Hz, 1H), 3.38 (t, J = 8.5 Hz, 1H), 3.30 (ddd, J = 9.8, 6.9, 2.2 Hz, 1H), 2.95–2.84 (m, 1H), 2.64–2.58 (m, 1H), 2.53 (ddd, J = 8.7, 3.7, 2.5 Hz, 1H), 2.01–1.89 (m, 2H), 1.79–1.65 (m, 1H), 1.60–1.45 ppm (m, 1H); ^{13}C NMR (75 MHz, $CDCl_3$): δ = 172.0, 161.9 (d, J = 244.7 Hz), 138.6, 137.4, 132.1, 130.8, 130.1 (d, J = 7.9 Hz), 129.8, 120.7, 118.5, 115.2 (d, J = 21.4 Hz), 70.8, 69.8, 65.9, 52.4, 51.4, 48.5, 43.4, 31.1, 24.7 ppm; ^{19}F NMR (282 MHz, $CDCl_3$): δ = −114.7 ppm (m, 1F); IR: $\tilde{\nu}$ = 2956, 2876, 1686, 1604, 1589, 1509, 1486, 1425, 1407, 1353, 1294, 1282, 1220, 1168, 1156, 1087, 1069, 1010 cm^{-1}; HRMS (MALDI): calculated for $C_{24}H_{25}BrFN_2O^+$ ([M+H]$^+$): 455.1129, found: 455.1122.

(1*RS*,3a*SR*,4*RS*,8a*SR*,8b*RS*)-4-(4-Bromophenyl)-1-difluoromethyl-2-(4-fluorobenzyl)octahydropyrrolo[3,4-*a*]pyrrolizin-3-one ((±)-25): *General procedure B*, starting from olefin (±)-**21** (569 mg, 1.25 mmol) and TFA (0.14 mL, 1.88 mmol) in CH_2Cl_2 (60 mL) gave aldehyde (±)-**24** (479 mg, 84%). *General procedure C*, starting from (±)-**24** (479 mg, 1.05 mmol) and DAST (806 mg, 5.00 mmol) gave (±)-**25** (97 mg, 16%) as a red solid. mp: 181–183 °C; ^{1}H NMR (300 MHz, $CDCl_3$): δ = 7.45, 7.28 (AA′BB′, J = 8.5 Hz, 4H), 7.19–7.15 (m, 2H), 7.02 (t, J = 8.7 Hz, 2H), 5.67 (dt, J = 55.4, 3.1 Hz, 1H), 4.86, 4.04 (AB, J = 15.2 Hz, 2H), 4.09 (d, J = 7.2 Hz, 1H), 3.52–3.44 (m, 1H), 3.37 (t, J = 7.5 Hz, 1H), 3.26–3.19 (m, 1H), 2.97–2.88 (m, 1H), 2.75–2.70 (m, 1H), 2.64–2.56 (m, 1H), 2.07–1.89 (m, 2H), 1.78–1.69 (m, 1H), 1.65–1.56 ppm (m, 1H); ^{13}C NMR (75 MHz, $CDCl_3$): δ = 172.7, 162.2 (d, J = 246.6 Hz), 137.8, 131.7 (d, J = 3.7 Hz), 130.8, 129.9 (d, J = 11.0 Hz), 120.9, 115.5 (d, J = 21.3 Hz), 114.8 (t, J = 245.4 Hz), 71.7, 69.8, 62.7 (t, J = 23.1 Hz), 52.1, 51.5, 44.7, 41.1, 31.5, 24.6 ppm; ^{19}F NMR (282 MHz, $CDCl_3$): δ = −126.7 (ddd, J = 289.1, 54.9, 10.7 Hz, 1 F), −125.5 (ddd, J = 288.3, 55.5, 12.7 Hz, 1F), −114.8 ppm (m, 1F); IR: $\tilde{\nu}$ = 2932, 2898, 2861, 2823, 1678, 1641, 1602, 1509, 1484, 1447, 1430, 1421, 1403, 1362, 1340, 1300, 1288, 1254, 1220, 1157, 1130, 1096, 1072, 1060, 1032, 1018, 1009 cm^{-1}; HRMS (MALDI): calculated for $C_{23}H_{23}BrF_3N_2O^+$ ([M+H]$^+$): 479.0940, found: 479.0935.

4-[(1*RS*,3a*SR*,4*RS*,8a*SR*,8b*RS*)-1-Difluoromethyl-2-(4-fluorobenzyl)-3-oxodecahydropyrrolo[3,4-*a*]pyrrolizin-4-yl]benzonitrile ((±)-26): *General procedure E*, starting from bromide (±)-**25** (189 mg, 0.39 mmol) and CuCN (141 mg, 1.58 mmol) in DMF (10 mL) gave (±)-**26** (71 mg, 42%) as a colorless solid. mp: 167–169 °C; ^{1}H NMR (300 MHz, $CDCl_3$): δ = 7.63, 7.53 (AA′BB′, J = 8.3 Hz, 4H), 7.19 (dd, J = 8.4, 5.3 Hz, 2H), 7.04 (dd, J = 8.7, 8.4 Hz, 2H), 5.69 (dt, J = 55.1, 3.1 Hz, 1H), 4.85, 4.04 (AB, J = 15.2 Hz, 2H), 4.18 (d, J = 6.9 Hz, 1H), 3.54–3.40 (m, 2H), 3.27–3.21 (m, 1H), 3.01–2.93 (m, 1H), 2.78–2.70 (m, 1H), 2.62–2.54 (m, 1H), 2.09–1.90 (m, 2H), 1.81–1.72 (m, 1H), 1.67–1.58 ppm (m, 1H); ^{13}C NMR (75 MHz, $CDCl_3$): δ = 172.7, 162.5 (d, J = 246.5 Hz), 145.1, 131.8, 130.0 (d, J = 8.1 Hz), 128.9, 119.4, 115.9 (d, J = 21.5 Hz), 115.0 (t, J = 246.3 Hz), 111.0, 72.0, 70.5, 62.8 (t, J = 23.7 Hz), 52.6, 52.1, 45.0, 41.4, 32.0, 25.1 ppm; ^{19}F NMR (282 MHz, $CDCl_3$): δ = −127.4 (ddd, J = 288.5, 54.9, 10.9 Hz, 1F), −125.9 (ddd, J = 288.5, 55.5, 12.9 Hz, 1F), −114.6 ppm (m, 1F); IR: $\tilde{\nu}$ = 2961, 2876, 2225, 1692, 1607, 1509, 1442, 1427, 1410, 1377, 1355, 1297, 1287, 1222, 1171, 1157, 1132, 1112, 1070, 1042, 1017 cm^{-1}; HRMS (MALDI): calculated for $C_{24}H_{23}F_3N_3O^+$ ([M+H]$^+$): 426.1788, found: 426.1781.

4-[(1*RS*,3a*SR*,4*RS*,8a*SR*,8b*RS*)-1-Difluoromethyl-2-(4-fluorobenzyl)-3-oxodecahydropyrrolo[3,4-*a*]pyrrolizin-4-yl]benzamidine hydrochloride ((±)-7): *General procedure F*, starting from nitrile (±)-**26** (64 mg, 0.15 mmol) in CH_2Cl_2 (0.9 mL) and MeOH (1.7 mL) gave (±)-**7** (49 mg, 68%) as a colorless solid. mp: 178–180 °C; ^{1}H NMR (300 MHz, CD_3OD): δ = 7.74, 7.65 (AA′BB′, J = 8.4 Hz, 4H), 7.33–7.28 (m, 2H), 7.10 (dd, J = 9.0, 8.7 Hz, 2H), 6.03 (dt, J = 55.0, 2.4 Hz, 1H), 4.80, 4.13 (AB, J = 15.2 Hz, 1H), 4.33 (d, J = 6.8 Hz, 1H), 3.74–3.66 (m, 1H), 3.55 (t, J = 7.3 Hz, 1H), 3.35–3.29 (m, 1H), 3.01–2.92 (m, 1H), 2.90–2.86 (m, 1H), 2.64–2.55 (m, 1H), 2.08–1.95 (m, 2H), 1.83–1.65 ppm (m, 2H); ^{13}C NMR (75 MHz, CD_3OD): δ = 175.2, 168.2, 163.6 (d, J = 243.3 Hz), 147.8, 133.1 (d, J = 3.2 Hz), 130.8 (d, J = 8.0 Hz), 130.0, 128.1, 127.7, 116.7 (t, J = 242.4 Hz), 116.3 (d, J = 21.7 Hz), 73.3, 71.2, 64.1 (t, J = 22.5 Hz), 53.5, 53.3, 45.6, 42.2, 32.3, 25.5 ppm; ^{19}F NMR (282 MHz, CD_3OD): δ = −129.6 (ddd, J = 287.9, 54.8, 12.6 Hz, 1F), −125.9 (ddd, J = 287.4, 55.3, 13.1 Hz, 1F), −115.6 ppm (m, 1F); IR: $\tilde{\nu}$ = 3256, 3060, 2951, 2879, 1668, 1611, 1538, 1510, 1489, 1445, 1435, 1414, 1377, 1357, 1310, 1287, 1221, 1158, 1108, 1070, 1040, 1016 cm^{-1}; HRMS (MALDI): calculated for $C_{24}H_{26}F_3N_4O^+$ ([M+H]$^+$): 443.2053, found: 443.2046.

(1*RS*,3a*SR*,4*RS*,8a*SR*,8b*RS*)-4-(4-Bromophenyl)-2-(4-fluorobenzyl)-1-(trifluoromethyl)octahydro-1-hydroxypyrrolo[3,4-*a*]-pyrrolizin-3-one ((±)-27): *General procedure G*, starting from imide (±)-**16** (222 mg, 0.5 mmol), CsF (8 mg, 0.05 mmol), and CF_3SiMe_3 (285 mg, 2 mmol) in THF (10 mL) gave (±)-**27** (164 mg, 64%) as a yellowish solid. mp: 75–78 °C; ^{1}H NMR (300 MHz, $CDCl_3$): δ = 7.37, 7.05 (AA′BB′, J = 8.4 Hz, 4H), 7.13 (dd, J = 8.4, 5.7 Hz, 2H), 6.90 (m, 2H), 5.83 (bs, 1H), 4.44, 4.22 (AB, J = 15.3 Hz, 2H), 3.94 (d, J = 10.8 Hz, 1H), 3.61–3.52 (m, 1H), 3.50 (m, 1H), 3.19 (d, J = 8.4 Hz, 1H), 3.01–2.91 (m, 1H), 2.83–2.75 (m, 1H), 2.17–2.01 (m, 2H), 1.96–1.84 (m, 1H), 1.71–1.57 ppm (m, 1H); ^{13}C NMR (75 MHz, $CDCl_3$): δ = 175.4, 161.2 (d, J = 243 Hz), 134.5, 132.8, 130.9, 129.7 (d, J = 8 Hz), 122.3 (q, J = 283 Hz), 121.1, 114.8 (d, J = 21 Hz), 90.4 (q, J = 33 Hz), 68.9, 67.4, 50.6, 49.3, 48.2, 42.2, 31.3, 26.2 ppm; ^{19}F NMR (282 MHz, $CDCl_3$): δ = −115.0 (m, 1F), −79.5 ppm (s, 3F); IR: $\tilde{\nu}$ = 3044, 2925, 1710, 1512, 1397, 1342, 1261, 1184, 1154, 1080 cm^{-1}; HRMS (MALDI): calculated for $C_{23}H_{22}BrF_4N_2O_2^+$ ([M+H]$^+$): 513.0795, found: 513.0807.

4-((1*RS*,3a*SR*,4*RS*,8a*SR*,8b*RS*)-2-(4-Fluorobenzyl)-1-hydroxy-3-oxo-1-(trifluoromethyl)decahydropyrrolo[3,4-*a*]pyrrolizin-4-yl)benzonitrile ((±)-28): *General procedure E*, starting from aryl bromide (±)-**27** (468 mg, 0.912 mmol) and CuCN (327 mg, 4 mmol) in DMF

 © 2006 Wiley-VCH Verlag GmbH & Co. KGaA, Weinheim

(5 mL) gave (±)-**28** (306 mg, 73%). mp: 144–145 °C; ^{1}H NMR (300 MHz, $CDCl_3$): δ = 7.51, 7.30 (AA′BB′, J = 8.1 Hz, 4H), 7.11 (dd, J = 8.4, 5.7 Hz, 2H), 6.88 (t, J = 8.4 Hz, 2H), 6.26 (bs, 1H), 4.39, 4.19 (AB, J = 15.3 Hz, 2H), 4.03 (d, J = 9.9 Hz, 1H), 3.63–3.57 (m, 1H), 3.53 (m, 1H), 3.20 (d, J = 8.4 Hz, 1H), 3.02–2.92 (m, 1H), 2.77–2.69 (m, 1H), 2.15–2.03 (m, 2H), 1.95–1.84 (m, 1H), 1.72–1.57 ppm (m, 1H); ^{13}C NMR (75 MHz, $CDCl_3$): δ = 172.7, 161.9 (d, J = 244 Hz), 142.6, 132.6, 131.9, 130.3, 128.5, 123.3 (q, J = 284 Hz), 118.5, 114.6 (d, J = 21 Hz), 111.5, 88.9 (q, J = 32 Hz), 66.6, 66.2, 50.7, 48.4, 45.4, 43.0, 26.8, 22.8 ppm; ^{19}F NMR (282 MHz, $CDCl_3$): δ = −114.8 (m, 1F), −79.6 ppm (s, 3F); IR: $\tilde{\nu}$ = 3632, 3080, 2976, 2889, 2232, 1705, 1610, 1509, 1463, 1387, 1343, 1308, 1221, 1176, 1156, 1145, 1087, 1073, 1004 cm^{-1}; HRMS (MALDI): calculated for $C_{24}H_{22}F_4N_3O_2^+$ ([M+H]$^+$): 460.1648, found: 460.1636.

4-[(1*RS*,3a*SR*,4*RS*,8a*SR*,8b*RS*)-2-(4-Fluorobenzyl)-1-hydroxy-3-oxo-1-(trifluoromethyl)decahydropyrrolo[3,4-*a*]pyrrolizin-4-yl]benzamidine hydrochloride ((±)-10): *General procedure F*, starting from nitrile (±)-**28** (188 mg, 0.41 mmol) in CH_2Cl_2 (1.0 mL) and MeOH (2.0 mL) gave (±)-**10** (103 mg, 53%) as a colorless solid. mp: 162–164 °C (dec); ^{1}H NMR (300 MHz, CD_3OD): δ = 7.70, 7.27 (AA′BB′, J = 8.1 Hz, 4H), 7.12 (dd, J = 8.7, 5.7 Hz, 2H), 6.88 (t, J = 8.7 Hz, 2H), 6.33 (bs, 2H), 6.00 (bs, 2H), 4.39, 4.25 (AB, J = 15.3 Hz, 2H), 4.05 (d, J = 10.5 Hz, 1H), 3.68–3.60 (m, 1H), 3.55 (t, J = 9.9 Hz, 1H), 3.21 (d, J = 8.4, 1H), 3.03–2.93 (m, 1H), 2.82–2.73 (m, 1H), 2.21–2.02 (m, 2H), 1.96–1.85 (m, 1H), 1.75–1.62 ppm (m, 1H); ^{13}C NMR (75 MHz, CD_3OD): δ = 173.5, 167.1, 162.1 (d, J = 242.3 Hz), 146.5, 133.6, 129.2 (d, J = 7.9 Hz), 129.0, 127.1, 126.8, 124.8 (q, J = 292.7 Hz), 114.5 (d, J = 21.8 Hz), 88.4 (q, J = 31.0 Hz), 70.3, 64.7, 52.8, 51.8, 42.6, 31.0, 24.3 ppm; ^{19}F NMR (282 MHz, CD_3OD): δ = −118.0 (m, 1F), −82.6 ppm (s, 3F); IR: $\tilde{\nu}$ = 3322, 3016, 2530, 2470, 1711, 1684, 1664, 1512, 1446, 1410, 1380, 1340, 1283, 1266, 1229, 1185, 1164, 1145, 1102, 1076, 1019, 1006 cm^{-1}; HRMS (MALDI): calculated for $C_{24}H_{25}F_4N_4O_2^+$ ([M+H]$^+$): 477.1908, found: 477.1904.

4-((1*RS*,3a*SR*,4*RS*,8a*SR*,8b*RS*)-1-Fluoro-2-(4-fluorobenzyl)-3-oxo-1-(trifluoromethyl)decahydropyrrolo[3,4-*a*]pyrrolizin-4-yl)benzonitrile ((±)-29) and 4-((1*SR*,3a*SR*,4*RS*,8a*SR*,8b*RS*)-1-Fluoro-2-(4-fluorobenzyl)-3-oxo-1-(trifluoromethyl)decahydropyrrolo[3,4-*a*]pyrrolizin-4-yl)benzonitrile ((±)-30): *General procedure C*, starting from (±)-**28** (140 mg, 0.31 mmol) and DAST (98 mg, 0.61 mmol) gave (±)-**29** (62 mg, 43%) and (±)-**30** (57 mg, 40%) as yellowish solids.

Data for (±)-29: mp: 125–127 °C; ^{1}H NMR (300 MHz, $CDCl_3$): δ = 7.53, 7.41 (AA′BB′, J = 8.4 Hz, 4H), 7.15 (dd, J = 8.7, 5.4 Hz, 2H), 6.96 (t, J = 8.7 Hz, 2H), 4.53 (d, J = 15.6 Hz, 1H), 4.32 (dd, J = 15.6, 2.1 Hz, 1H), 4.16 (d, J = 8.1 Hz, 1H), 3.83 (t, J = 8.4 Hz, 1H), 3.51 (dt, J = 8.6, 2.4 Hz, 1H), 3.20 (dt, J = 7.2, 1.8 Hz, 1H), 3.01–2.92 (m, 1H), 2.67–2.58 (m, 1H), 2.15–1.96 (m, 2H), 1.88–1.73 (m, 1H), 1.72–1.58 ppm (m, 1H); ^{13}C NMR (75 MHz, $CDCl_3$): δ = 172.2, 162.1 (d, J = 244.0 Hz), 144.0, 131.7, 129.8 (d, J = 7.9 Hz), 128.8, 121.8 (dq, J = 284.1, 48.5 Hz), 118.9, 115.1 (d, J = 21.3 Hz), 111.2, 102.3 (dq, J = 221.6, 34.7 Hz), 69.6, 64.5 (d, J = 11.6 Hz), 52.0, 50.7, 46.0 (d, J = 17.6 Hz), 43.6, 30.6, 24.1 ppm; ^{19}F NMR (282 MHz, $CDCl_3$): δ = −142.7 (m, 1F), −114.3 (m, 1F), −80.3 ppm (d, J = 7.3 Hz, 3F); IR: $\tilde{\nu}$ = 2975, 2884, 2227, 1727, 1608, 1512, 1444, 1388, 1344, 1293, 1273, 1253, 1215, 1182, 1156, 1142, 1116, 1100, 1058, 1027, 1019 cm^{-1}; HRMS (MALDI): calculated for $C_{24}H_{20}F_5N_3O^+$ ([M+H]$^+$): 462.1599, found: 462.1604.

Data for (±)-30: mp: 147–150 °C; ^{1}H NMR (300 MHz, $CDCl_3$): δ = 7.64, 7.53 (AA′BB′, J = 8.4 Hz, 4H), 7.18 (dd, J = 8.7, 5.4 Hz, 2H), 6.94 (t, J = 8.7 Hz, 2H), 4.56, 4.36 (AB, J = 15.6 Hz, 2H), 4.21 (d, J = 6.6 Hz, 1H), 3.77–3.69 (m, 1H), 3.54 (t, J = 6.6 Hz, 1H), 3.09 (ddd, J = 15.9, 7.4, 4.2 Hz, 1H), 3.03–2.94 (m, 1H), 2.63–2.54 (m, 1H), 2.19–2.08 (m, 1H), 2.06–1.93 (m, 1H), 1.89–1.74 (m, 1H), 1.73–1.60 ppm (m, 1H); ^{13}C NMR (75 MHz, $CDCl_3$): δ = 174.3, 162.5 (d, J = 244.7 Hz), 144.0, 132.1, 130.1 (d, J = 8.5 Hz), 129.1, 128.9, 121.5 (dq, J = 284.3, 43.8 Hz), 119.3, 115.4 (d, J = 21.2 Hz), 104.9 (dq, J = 215.0, 35.3 Hz), 69.1, 64.5, 52.4, 50.9, 50.2 (d, J = 27.8 Hz), 43.9, 32.1, 25.2 ppm; ^{19}F NMR (282 MHz, $CDCl_3$): δ = −116.2 (d, J = 14.9 Hz, 1F), −115.1 (m, 1F), −73.1 ppm (d, J = 4.5 Hz, 3F); IR: $\tilde{\nu}$ = 2963, 2879, 2235, 1741, 1608, 1512, 1448, 1416, 1385, 1345, 1316, 1300, 1262, 1207, 1167, 1155, 1120, 1109, 1098, 1062, 1021, 1011 cm^{-1}; HRMS (MALDI): calculated for $C_{24}H_{20}F_5N_3O^+$ ([M+H]$^+$): 462.1599, found: 462.1606.

4-((1*RS*,3a*SR*,4*RS*,8a*SR*,8b*RS*)-2-(4-Fluorobenzyl)-1-methoxy-3-oxo-1-(trifluoromethyl)decahydropyrrolo[3,4-*a*]pyrrolizin-4-yl)-benzonitrile ((±)-31): Nitrile (±)-**28** (133 mg, 0.29 mmol), 18-crown-6 (137, 0.52 mmol), and MeI (27.5 μL, 0.44 mmol) were dissolved in dry THF (5 mL) at 25 °C, then NaH (18 mg, 0.44 mmol, as a 60% emulsion in mineral oil) was slowly added (over 20 min). The mixture was stirred for 1 h, then a saturated aqueous NH_4Cl solution was added and the mixture extracted with AcOEt. The organic phases were dried (Na_2SO_4) and the solvent evaporated in vacuo. The residue was purified by CC (SiO_2; CH_2Cl_2/AcOEt 2:1) to give (±)-**31** in quantitative yield (137 mg) as a yellow solid. mp: 96–97 °C; ^{1}H NMR (300 MHz, $CDCl_3$): δ = 7.58, 7.46 (AA′BB′, J = 8.4 Hz, 4H), 7.19 (dd, J = 8.7, 5.3 Hz, 2H), 6.93 (t, J = 8.7 Hz, 2H), 4.43, 4.31 (AB, J = 15.5 Hz, 2H), 4.18 (d, J = 7.2 Hz, 1H), 3.81 (ddd, J = 9.3, 6.8, 2.8 Hz, 1H), 3.54 (s, 3H), 3.44 (dd, J = 8.4, 7.2 Hz, 1H), 3.15 (dd, J = 8.4, 2.8 Hz, 1H), 3.02–2.92 (m, 1H), 2.66–2.56 (m, 1H), 2.21–2.09 (m, 1H), 2.08–1.96 (m, 1H), 1.91–1.66 ppm (m, 2H); ^{13}C NMR (75 MHz, CD_3OD): δ = 172.0, 161.8 (d, J = 243.5 Hz), 144.2, 132.6, 131.6, 129.1 (d, J = 7.9 Hz), 128.6, 123.8 (q, J = 290.3 Hz), 119.0, 114.8 (d, J = 21.2 Hz), 111.0, 92.5 (q, J = 29.8 Hz), 70.1, 64.4, 53.3, 52.1, 51.4, 45.7, 43.3, 31.7, 24.4 ppm; ^{19}F NMR (282 MHz, CD_3OD): δ = −115.6 (m, 1F), −76.6 ppm (s, 3F); IR: $\tilde{\nu}$ = 2951, 2924, 2848, 2225, 1712, 1607, 1510, 1460, 1429, 1387, 1339, 1314, 1300, 1266, 1215, 1156, 1133, 1097, 1043, 1017 cm^{-1}; HRMS (MALDI): calculated for $C_{25}H_{24}F_4N_3O_2^+$ ([M+H]$^+$): 474.1790, found: 474.1799.

4-((1*RS*,3a*SR*,4*RS*,8a*SR*,8b*RS*)-2-(4-Fluorobenzyl)-1-methoxy-3-oxo-1-(trifluoromethyl)decahydropyrrolo[3,4-*a*]pyrrolizin-4-yl)-benzamidine hydrochloride ((±)-11): *General procedure F*, starting from nitrile (±)-**31** (74 mg, 0.16 mmol) in CH_2Cl_2 (0.8 mL) and MeOH (1.6 mL) gave (±)-**11** (40 mg, 51%) as a colorless solid. mp: 183–186 °C (dec); ^{1}H NMR (300 MHz, $CDCl_3$): δ = 8.68 (bs, 2H), 8.56 (bs, 2H), 7.71, 7.36 (AA′BB′, J = 8.1 Hz, 4H), 7.08 (dd, J = 8.1, 5.7 Hz, 2H), 6.89 (t, J = 8.7 Hz, 2H), 4.32, 4.26 (AB, J = 16.5 Hz, 2H), 4.13 (d, J = 7.8 Hz, 1H), 3.84–3.76 (m, 1H), 3.55 (s, 3H), 3.44 (t, J = 7.2 Hz, 1H), 3.18–3.14 (m, 1H), 2.87–2.78 (m, 1H), 2.47–2.39 (m, 1H), 2.22–1.90 (m, 2H), 1.85–1.71 ppm (m, 2H); ^{13}C NMR (75 MHz, CD_3OD): δ = 173.0, 165.2, 161.7 (d, J = 244.2 Hz), 145.3, 132.4, 128.9 (d, J = 7.9 Hz), 128.3, 127.9, 125.7, 123.8 (q, J = 293.3 Hz), 115.0 (d, J = 21.2 Hz), 92.7 (q, J = 29.1 Hz), 69.9, 64.1, 53.7, 52.8, 51.4, 45.6, 43.5, 32.0, 24.7 ppm; ^{19}F NMR (282 MHz, CD_3OD): δ = −114.9 (m, 1F), −75.9 ppm (s, 3F); IR: $\tilde{\nu}$ = 3266, 3204, 3064, 2956, 2879, 1675, 1610, 1539, 1510, 1487, 1434, 1395, 1352, 1334, 1314, 1297, 1267, 1218, 1166, 1157, 1134, 1097, 1034, 1017 cm^{-1}; HRMS (MALDI): calculated for $C_{25}H_{27}F_4N_4O_2^+$ ([M+H]$^+$): 491.2190, found: 491.2182.

4-[(1*SR*,3a*SR*,4*RS*,8a*SR*,8b*RS*)-2-(4-Fluorobenzyl)-1-methoxy-3-oxo-1-(trifluoromethyl)decahydropyrrolo[3,4-*a*]pyrrolizin-4-yl]-benzamidine hydrochloride ((±)-12): *General procedure F*, starting from nitrile (±)-**29** (100 mg, 0.22 mmol) in CH_2Cl_2 (1.5 mL) and MeOH (0.5 mL) gave (±)-**12** (44 mg, 41%) as a yellowish foam. mp. 64–66 °C (dec); ^{1}H NMR (300 MHz, $CDCl_3$): δ = 9.20–8.20 (bs, 4H),

 © 2006 Wiley-VCH Verlag GmbH & Co. KGaA, Weinheim

7.84, 7.56, (AA'BB', $J=8.7$ Hz, 4H), 6.99 (dd, $J=8.1$, 5.7 Hz, 2H), 6.83 (dd, $J=8.7$, 8.1 Hz, 2H), 4.26 (s, 2H), 4.12 (d, $J=6.3$ Hz, 1H), 3.80–3.72 (m, 1H), 3.54 (t, $J=7.2$ Hz, 1H), 2.96 (s, 3H), 2.98–2.92 (m, 1H), 2.79–2.64 (m, 1H), 2.39–2.26 (m, 1H), 2.14–2.00 (m, 1H), 1.93–1.82 (m, 1H), 1.75–1.59 ppm (m, 2H); ^{13}C NMR (75 MHz, $CDCl_3$): $\delta=$ 175.3, 165.8, 162.3 (d, $J=245.4$ Hz), 145.9, 131.7, 130.3 (d, $J=$ 7.9 Hz), 129.1, 128.2, 126.1, 123.0 (q, $J=285.5$ Hz), 115.4 (d, $J=$ 21.2 Hz), 94.7 (q, $J=31.0$ Hz), 68.4, 65.5, 52.3, 51.3, 50.2, 47.5, 43.8, 32.0, 24.1 ppm; ^{19}F NMR (282 MHz, $CDCl_3$): $\delta=-113.8$ (m, 1F), -71.0 ppm (s, 3F); IR: $\tilde{\nu}=3323$, 3109, 2941, 2873, 2646, 1654, 1638, 1608, 1579, 1509, 1489, 1397, 1308, 1259, 1244, 1220, 1176, 1154, 1117, 1084, 1013 cm^{-1}; HRMS (MALDI): calculated for $C_{25}H_{27}F_4N_4O_2^+$ ($[M+H]^+$): 491.2065, found: 491.2059.

X-ray analysis: The structures were solved by direct methods (SIR97)[26] and refined by full-matrix least-squares analysis (SHELXL-97),[27] using an isotropic extinction correction. All non H-atoms were refined anisotropically, H-atoms isotropically, whereby H-positions are based on stereochemical considerations. For summaries of the small-structure X-ray analyses, see SI.

X-ray crystal structure of the complex of thrombin with (+)-7: Diffraction data were measured at the Swiss Light Source (SLS) on beamline PXII. The wavelength was 0.91954 Å, the detector MarCCD225 at 100 mm, and exposure times were 1 s for 513 frames of 0.4°. The images showed strong ice rings and ~100 overloads per image. A second low resolution (2.2 Å) run was performed with the detector at 250 mm, and an extra Al filter. A total of 180 frames of 1° were measured. The data were processed to 1.31 Å resolution using XDS, including the 'zero dose' radiation damage correction with default values. The space group is *C*2 with unit cell dimensions $a=70.64$ Å, $b=71.41$ Å, $c=72.52$ Å, $\beta=$ 100.35°. For 391661 observations of 83900 reflections, (with ice rings excluded 2.28–2.22 Å, 1.97–1.93 Å, and 1.465–1.45 Å) the merging *R* factor on intensities was 6.8% (36.9% in the outermost shell, 1.37–1.3 Å), with completeness 96.4% (100%) and I/σ 14.2 (5.1). Data reduction used the CCP4 package.[28] High *R* factors on the ice ring edges required further deletion of reflections in the resolution ranges 1.465–1.45 Å and 1.93–1.89 Å and an outer cutoff of 1.305 Å. Refinement with Refmac5[29] used the TLS option and hydrogens were inserted at riding positions, where unique. The final overall crystallographic *R* factors are 18.4% (working) and 20.4% (free), with values in the outer shell (1.334–1.305 Å) of 25.0% and 26.0%, respectively, for 79708 (4196) reflections and 2789 non-hydrogen atoms, including one Na^+ ion, one Ca^{++} ion, and 397 water molecules. Seven residues were given alternative conformations. The inhibitor density is very clear. Coordinates have been deposited at the Protein Data Bank, PDB code: 2CN0.

Acknowledgements

This research was supported by F. Hoffmann-La Roche Ltd, Chugai Pharmaceuticals, and the ETH Research Council. A.H.-R. thanks the Deutsche Forschungsgemeinschaft (Emmy Noether-Programm). We thank Olivier Kuster, Dr. Thomas Tschopp, and Dr. Alain Gast for the biological assays and Tobias Platen for his help in the preparation of some compounds.

Keywords: distribution coefficient · enzyme inhibitors · fluorine · noncovalent interactions · pK_a values · thrombin

[1] a) K. Johns, G. Stead, *J. Fluorine Chem.* **2000**, *104*, 5–18; b) P. Jeschke, *ChemBioChem* **2004**, *5*, 570–589; c) H.-J. Böhm, D. Banner, S. Bendels, M. Kansy, B. Kuhn, K. Müller, U. Obst-Sander, M. Stahl, *ChemBioChem* **2004**, *5*, 637–643; d) W. R. Dolbier, Jr., *J. Fluorine Chem.* **2005**, 126, 157–163; e) F. Leroux, P. Jeschke, M. Schlosser, *Chem. Rev.* **2005**, *105*, 827–856.

[2] a) *Organofluorine Chemistry, Principles and Commercial Applications* (Eds.: R. E. Banks, B. E. Smart, J. C. Tatlow), Plenum, New York, **1994**; b) P. Kirsch, *Modern Fluoroorganic Chemistry: Synthesis Reactivity, Applications*, Wiley-VCH, Weinheim, **2004**.

[3] a) D. O'Hagan, H. S. Rzepa, *Chem. Commun.* **1997**, 645–652; b) B. E. Smart, *J. Fluorine Chem.* **2001**, *109*, 3–11; c) K. Mikami, Y. Itoh, M. Yamanaka, *Chem. Rev.* **2004**, *104*, 1–16.

[4] a) F. M. D. Ismail, *J. Fluorine Chem.* **2002**, *118*, 27–33; b) C. Isanbor, D. O'Hagan, *J. Fluorine Chem.* **2006**, *127*, 303–319.

[5] a) J. A. Olsen, D. W. Banner, P. Seiler, U. Obst Sander, A. D'Arcy, M. Stihle, K. Müller, F. Diederich, *Angew. Chem.* **2003**, *115*, 2611–2615; *Angew. Chem. Int. Ed.* **2003**, *42*, 2507–2511; b) J. A. Olsen, D. W. Banner, P. Seiler, B. Wagner, T. Tschopp, U. Obst-Sander, M. Kansy, K. Müller, F. Diederich, *ChemBioChem* **2004**, *5*, 666–675; c) J. Olsen, P. Seiler, B. Wagner, H. Fischer, T. Tschopp, U. Obst-Sander, D. W. Banner, M. Kansy, K. Müller, F. Diederich, *Org. Biomol. Chem.* **2004**, *2*, 1339–1352.

[6] a) U. Obst, V. Gramlich, F. Diederich, L. Weber, D. W. Banner, *Angew. Chem.* **1995**, *107*, 1874–1877; *Angew. Chem. Int. Ed. Engl.* **1995**, *34*, 1739–1742; b) U. Obst, D. W. Banner, L. Weber, F. Diederich, *Chem. Biol.* **1997**, *4*, 287–295; c) K. Schärer, M. Morgenthaler, P. Seiler, F. Diederich, D. W. Banner, T. Tschopp, U. Obst-Sander, *Helv. Chim. Acta* **2004**, *87*, 2517–2538; d) J. Fokkens, G. Klebe, *Angew. Chem.* **2006**, *118*, 1000–1004; *Angew. Chem. Int. Ed.* **2006**, *45*, 985–989.

[7] R. Paulini, K. Müller, F. Diederich, *Angew. Chem.* **2005**, *117*, 1820–1839; *Angew. Chem. Int. Ed.* **2005**, *44*, 1788–1805.

[8] E. Schweizer, A. Hoffmann-Röder, J. A. Olsen, U. Obst-Sander, B. Wagner, M. Kansy, D. W. Banner, F. Diederich, *Org. Biomol. Chem.* **2006**, *4*, 2364–2375.

[9] E. Schweizer, A. Hoffmann-Röder, K. Schärer, J. A. Olsen, C. Fäh, P. Seiler, U. Obst-Sander, B. Wagner, M. Kansy, F. Diederich, *ChemMedChem*. **2006**, *1*, 611–621.

[10] In related studies on halogenated phenylamidinium residues, the loss in binding affinity was attributed to steric effects: a) R. L. Mackman, B. A. Katz, J. G. Breitenbucher, H. C. Hui, E. Verner, C. Luong, L. Liu, P. A. Sprengeler, *J. Med. Chem.* **2001**, *44*, 3856–3871; b) B. A. Katz, P. A. Sprengeler, C. Luong, E. Verner, K. Elrod, M. Kirtley, J. Janc, J. R. Spencer, J. G. Breitenbucher, H. Hui, D. McGee, D. Allen, A. Martelli, R. L. Mackman, *Chem. Biol.* **2001**, *8*, 1107–1121.

[11] a) A. Pinner, F. Klein, *Ber. Dtsch. Chem. Ges.* **1877**, *10*, 1889–1897; b) G. Wagner, I. Wunderlich, *Pharmazie* **1977**, *32*, 76–79.

[12] W. J. Middleton, *J. Org. Chem.* **1975**, *40*, 574–578.

[13] a) A. A. Kolomeitsev, V. N. Movchun, Y. L. Yagupolskii, J. Porwisiak, W. Dmowski, *Tetrahedron Lett.* **1992**, *33*, 6191–6192; b) D. V. Sevenard, P. Kirsch, G.-V. Röschenthaler, V. N. Movchun, A. A. Kolomeitsev, *Synlett* **2001**, 379–382.

[14] a) I. Ruppert, K. Schlich, W. Volbach, *Tetrahedron Lett.* **1984**, *25*, 2195–2198; b) G. K. S. Prakash, A. K. Yudin, *Chem. Rev.* **1997**, *97*, 757–786; c) R. P. Singh, J. M. Shreeve, *Tetrahedron* **2000**, *56*, 7613–7632; d) G. K. S. Prakash, M. Mandal, *J. Fluorine Chem.* **2001**, *112*, 123–131; e) B. R. Langlois, T. Billard, *Synthesis* **2003**, 185–194; f) J.-A. Ma, D. Cahard, *Chem. Rev.* **2004**, *104*, 6119–6146; g) B. R. Langlois, T. Billard, S. Roussel, *J. Fluorine Chem.* **2005**, *126*, 173–179; h) S. Mizuta, N. Shibata, T. Sato, H. Fujimoto, S. Nakamura, T. Toru, *Synlett* **2006**, 267–279.

[15] A. Hoffmann-Röder, P. Seiler, F. Diederich, *Org. Biomol. Chem.* **2004**, *2*, 2267–2270.

[16] The *exo* selectivity of the addition was confirmed by X-ray analysis for differently substituted scaffolds, see Supporting Information.

[17] R. Krishnamurti, D. R. Bellew, G. K. S. Prakash, *J. Org. Chem.* **1991**, *56*, 984–989.

[18] a) D. J. Burton, Z.-Y. Yang, *Tetrahedron* **1992**, *48*, 189–275; b) S. Lavaire, R. Plantier-Royon, C. Portella, *Tetrahedron: Asymmetry* **1998**, *9*, 213–226; c) U. Eilitz, C. Böttcher, L. Hennig, A. Haas, C. Boyer, K. Burger, *J. Fluorine Chem.* **2002**, *115*, 149–154.

[19] Nucleophilic perfluoroalkylation of nitrile substituted tricyclic imides also proceeded smoothly. However, we did not pursue this route fur-

 © 2006 Wiley-VCH Verlag GmbH & Co. KGaA, Weinheim

ther since the final Pinner reaction would have interfered with the lability of the perfluoroalkylated lactam entity.

[20] a) T. Katagiri, H. Ihara, M. Takahashi, S. Kashino, K. Furuhashi, K. Uneyama, *Tetrahedron: Asymmetry* **1997**, *8*, 2933 – 2937; b) T. Katagiri, M. Irie, K. Uneyama, *Tetrahedron: Asymmetry* **1999**, *10*, 2583 – 2589; c) F. Grellepois, F. Chorki, B. Crousse, M. Ourévitch, D. Bonnet-Delpon, J.-P. Bégué, *J. Org. Chem.* **2002**, *67*, 1253 – 1260; d) G. Magueur, B. Crousse, M. Ourévitch, J.-P. Bégué, D. Bonnet-Delpon, *J. Org. Chem.* **2003**, *68*, 9763 – 9766; e) T. Katagiri, K. Uneyama, *Chirality* **2003**, *15*, 4 – 9.

[21] a) P. R. Gerber, K. Müller, *J. Comput.-Aided Mol. Des.* **1995**, *9*, 251 – 268; b) Gerber Molecular Design (http://www.moloc.ch).

[22] a) R. Lottenberg, J. A. Hall, M. Blinder, E. P. Binder, C. M. Jackson, *Biochim. Biophys. Acta* **1983**, *742*, 539 – 557; b) K. Hilpert, J. Ackermann, D. W. Banner, A. Gast, K. Gubernator, P. Hadváry, L. Labler, K. Müller, G. Schmid, T. B. Tschopp, H. van de Waterbeemd, *J. Med. Chem.* **1994**, *37*, 3889 – 3901.

[23] In a recent study, a CF_3 group was found to act as an effective bioisoster for an isobutyl group within a lipophilic binding pocket: C. Binkert, M. Frigerio, A. Jones, S. Meyer, C. Pesenti, L. Prade, F. Viani, M. Zanda, *ChemBioChem* **2006**, *7*, 181 – 186.

[24] M. Schlosser, *Angew. Chem.* **1998**, *110*, 1538 – 1556; *Angew. Chem. Int. Ed.* **1998**, *37*, 1496 – 1513.

[25] ACD/pK_a version 8.19. Head Office, Advanced Chemistry Development, Inc. 110 Yonge Street, 14th floor, Toronto, Ontario, Canada M5C 1T4.

[26] A. Altomare, M. C. Burla, M. Camalli, G. L. Cascarano, C. Giacovazzo, A. Guagliardi, A. G. G. Moliterni, G. Polidori, R. Spagna, *J. Appl. Crystallogr.* **1999**, *32*, 115 – 119.

[27] G. M. Sheldrick, *SHELXL-97 Program for the Refinement of Crystal Structures*, University of Göttingen, Germany, **1997**.

[28] Collaborative Computational Project, Number 4, *Acta Crystallogr. Sect. D* **1994**, *50*, 760 – 763.

[29] G. N. Murshudov, A. A. Vagin, E. J. Dodson, *Acta Crystallogr. Sect. D* **1997**, *53*, 240 – 255.

Received: May 22, 2006
Revised: July 22, 2006
Published online on September 26, 2006

 © 2006 Wiley-VCH Verlag GmbH & Co. KGaA, Weinheim